

Controlling Random Waves with Digital Building Blocks Based on Supersymmetry

Sunkyu Yu, Xianji Piao, and Namkyoo Park*

*Photonic Systems Laboratory, Department of Electrical and Computer Engineering,
Seoul National University, Seoul 08826, Korea*

(Received 21 March 2017; revised manuscript received 13 August 2017; published 6 November 2017)

Harnessing multimode waves allows high information capacity through modal expansions. Although passive multimode devices for broadband responses have been demonstrated in momentum or frequency domains, the difficulty in achieving collective manipulation of all eigenmodes has hindered the implementation of digital multimode devices such as switching. Here we propose building blocks for digital switching of spatially random waves based on parity-converted supersymmetric pairs of multimode potentials. We reveal that unbroken supersymmetric transformations of any parity-symmetric potential derive the parity reversal of all eigenmodes, which allows the complete isolation of random waves in the “off” state. With two representative solvable potentials, building blocks for binary and many-valued logics are then demonstrated for random waves: a harmonic pair for binary switching of arbitrary wave fronts and a Pöschl-Teller pair for multilevel switching which implements fuzzy membership functions. Our results realizing the transfer of arbitrary wave fronts between wave elements will lay the foundation of high-bandwidth data processing.

DOI: [10.1103/PhysRevApplied.8.054010](https://doi.org/10.1103/PhysRevApplied.8.054010)

I. INTRODUCTION

Digital electronics of today has been established upon stable switching operation of transistors [1], which is based on charge-density-based processing of electric signals. The current flow inside a transistor is controlled by a field exerted on the charge which is the density of electric wave functions independent of their phase information. The performance of electronic switching is, thus, insensitive to spatial profiles and phases of wave functions, allowing a high degree of freedom for information capacity.

However, the operation principle of digital photonics is disparate from the electronic one due to the lack of charges in photons. In contrast to the direct control of electrons with external fields, the control of light flows is, thus, achieved indirectly through the alteration of optical wave functions from light-matter interactions, which enforces strong modal dependence on optical modulations. This limit has hindered consistent and collective manipulations of multimodes in photonics, and, therefore, in spite of the success of passive multimode devices [2–6], most of the switching technologies in optics [7–10] have remained in single-mode operation with fixed input profiles, not only restricting information capacity but also enforcing the use of large-footprint multi-to-single-mode couplers [11–13]. To exploit the highest degree of freedom through multimode expansions and, thus, achieve high information capacity of light as observed in the bandwidth explosion with the introduction of waveform transparent optical amplifiers [14], the present obstacle for

collective switching of multimodes insensitive to spatial profiles of wave functions must be overcome.

In this paper, we propose the “building block” for the switching of “random” waves to realize digital photonic systems of high information capacity. To achieve collective and high contrast switching of multimodes contained within random waves, we employ the concept of supersymmetry (SUSY), which derives isospectrally transformed eigenmodes with the ground-state annihilation [15]. As a physical building block for the binary switching of random waves, we design a SUSY harmonic pair [15] possessing even-spacing, isospectral eigensystems, and most critically, having parity-reversed eigenmodes. By employing a pair of harmonic index profile waveguides and applying index modulations [16], the collective switching of multimodes is achieved, completely regenerating arbitrary wave fronts between optical elements without any loss of spatial information. With a SUSY Pöschl-Teller pair [15], we also demonstrate the multilevel switching [17], establishing a random wave membership function for many-valued fuzzy logics [18]. Our results extending the regime of digital photonics to random light conditions implement uncorrupted information transfer between elements and pave the way for fuzzy photonics [19].

II. BUILDING BLOCK FOR RANDOM WAVES

A. Basic concept

We start with the collective control of random waves (Fig. 1). To realize the switching of broadband spatial information, it is noted that conventional designs [7–10] require multiple switches with multiplexers and demultiplexers

*nkpark@snu.ac.kr

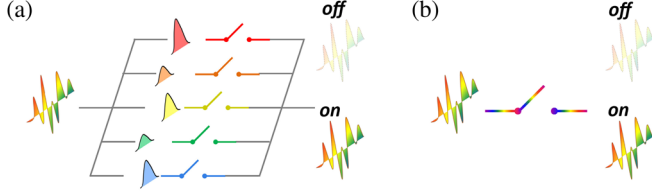


FIG. 1. The operation principle of controlling random waves. (a) Conventional operation composed of multiplexer, demultiplexer, and multiple single-mode switches. (b) A switching building block for random waves with the modal-profile-independent operation.

[Fig. 1(a)] for the separate switching of each participating mode. As an alternative, we propose a building block for the collective multimode switching [Fig. 1(b)], transparent to the spatial profiles and phases of the data.

B. Design criteria

Figure 2 shows the implementation of the building block for the mode-independent binary switching of random waves. For transverse-electric-mode propagating waves,

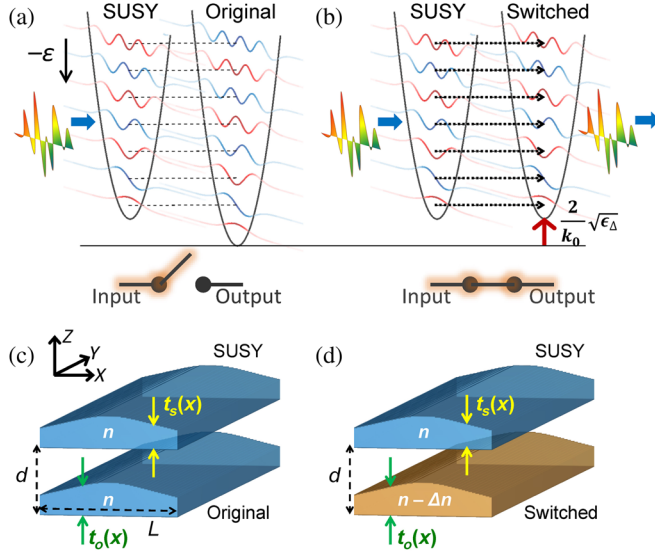


FIG. 2. The building block for digital binary switching of random waves: the SUSY harmonic pair. (a) *Off* state from the parity-reversed decoupling between the harmonic potential (output) and its SUSY partner (input). (b) *On* state from the parity-aligned coupling (black dotted arrows) through the modulation of the output potential (red arrow $\Delta\varepsilon = 2\varepsilon_\Delta^{1/2}/k_0$). The shapes of the eigenmodes are plotted on the potentials (red, even parity; blue, odd parity) in (a),(b). The configuration of the designed silicon waveguides is shown in (c) for the *off* state and (d) for the *on* state. The silicon refractive index is $n = 3.5$ at $\lambda_0 = 2\pi/k_0 = 1500$ nm. The “effective” relative permittivities for the original and SUSY-partner harmonic waveguide are $\varepsilon_o(x) = [10.38 - 7.48 \times 10^{-4}(k_0x)^2]$ and $\varepsilon_s(x) = [10.32 - 7.48 \times 10^{-4}(k_0x)^2]$, respectively. The waveguide width $L = 24.84$ μm , and the distance between the waveguides is $d = 800$ nm.

input and output ports are one-dimensional potentials represented by the Schrödinger-like equation $H\psi = \gamma\psi$ [20–22], where the Hamiltonian is $H = -(1/k_0^2)\partial_x^2 - \varepsilon(x)$, where $\varepsilon(x)$ is the relative permittivity, and k_0 is the free-space wave number. To achieve the modal independence, two criteria should be satisfied for eigenvalues and eigenmodes. First, we enforce eigenspectra in input and output potentials to be “*equally spaced*” and “*identical*” for simultaneous transitions of all the participating modes [Figs. 2(a) and 2(b)], to attain the global phase matching of multimodes: both at the *on* and *off* states. While *equally spaced* spectra can be obtained by employing the harmonic or Wannier-Stark ladder [23] potentials, the *identical* spectra, also known as isospectrality [24], can be implemented through the SUSY transformation [4,15,21,22,25–27].

Second, the mode overlap between ports is critical to both the isolation (*off*) and transparency (*on*) in switching. To achieve perfect isolation in the *off* state, all eigenmodes in input and output potentials should be decoupled, with zero modal overlap. To satisfy the two criteria, the isospectrality with equally spaced spectra, and perfectly decoupled eigenmodes, we introduce the “parity-reversed contact” [28] of input and output potentials having spectrally matched but globally parity-reversed eigenmodes [Fig. 2(a)].

C. Parity-reversed contact from SUSY

While the “equal-spacing isospectral” contact can be achieved by employing harmonic potentials with the concept of SUSY [4,15,21,22,25–27] based on the Darboux transformation [29], the necessity of “collective” parity conversion has not been explored before, to our knowledge. We, thus, start from Darboux transformation, focusing on the transformation of the eigenmodes.

In the Darboux transformation, the Hamiltonian is factorized as $H - \gamma_d = A^\dagger A$ where γ_d is a scalar constant. The operator A then becomes $A = (1/k_0)\partial_x + V(x)$ with the Riccati equation of $\partial_x V = k_0 V^2 + k_0[\varepsilon(x) + \gamma_d]$ for the superpotential $V(x)$. The particular solution of the equation for the “nonsingular” superpotential $V(x)$ is obtained as $V(x) = -(1/k_0)\partial_x \psi_d(x)/\psi_d(x)$, where ψ_d is the nodeless eigenmode of $H\psi_d = \gamma_d \psi_d$ from $\gamma_d \leq \gamma_0$, for the ground state of $H\psi_0 = \gamma_0 \psi_0$.

The isospectral SUSY-partner Hamiltonian $H_s = AA^\dagger + \gamma_d$ is then achieved with transformed eigenmode $A\psi$, from $AH\psi = (AA^\dagger A + \gamma_d A)\psi = (AA^\dagger + \gamma_d)A\psi = H_s(A\psi) = \gamma(A\psi)$. It is known that the condition of $\gamma_d = \gamma_0$ and $\psi_d = \psi_0$ provides the “unbroken” SUSY Hamiltonian for the bosonic (ψ) and fermionic ($A\psi$) relation with the ground-state annihilation ($A\psi_0 = 0$) [15], while $\gamma_d < \gamma_0$ results in the broken SUSY [30]. The unbroken SUSY partner $H_s = AA^\dagger + \gamma_0$, thus, becomes

$$H_s = -\frac{1}{k_0^2} \frac{d^2}{dx^2} - \left[\varepsilon(x) + \frac{2}{k_0^2} \frac{d}{dx} \left(\frac{\partial_x \psi_0}{\psi_0} \right) \right], \quad (1)$$

which leads to SUSY-transformed eigenmodes $\psi_s(x) = A\psi(x)$ and optical potential $\varepsilon_s(x) = \varepsilon(x) + (2/k_0^2)\partial_x[\partial_x\psi_0(x)/\psi_0(x)]$.

Having summarized the fundamentals of SUSY, we now proceed to construct multimodal ‘‘parity conversion’’ by applying the unbroken SUSY transformation to ‘‘parity-symmetric’’ potentials. For the parity operator P with $Pf(x) = f(-x)$, a parity-symmetric potential $\varepsilon(x) = \varepsilon(-x)$ satisfies the commutation $[H, P] = 0$, imposing the definite parity on all eigenmodes as $\psi(x) = \pm\psi(-x)$. Because the ground state ψ_0 is nodeless, only the even parity is allowed for $\psi_0(x)$ with $\varepsilon(x) = \varepsilon(-x)$. Then, the unbroken SUSY operator $A = (1/k_0)[\partial_x - \partial_x\psi_0(x)/\psi_0(x)]$ composed of $\partial_{-x} = -\partial_x$ and even ground state $\psi_0(x) = \psi_0(-x)$ leads to the parity reversal of all eigenmodes when applied to an original potential of even parity ($\varepsilon(x) = \varepsilon(-x)$). We note that the resulting unbroken SUSY corresponds to parity-reversed bosonic and fermionic states with ground-state annihilation, and this ‘‘collective parity conversion’’ with the isospectrality can be applied to *any* parity-symmetric potential $\varepsilon(x) = \varepsilon(-x)$ when unbroken SUSY transformation is applied (see Appendix A for the breaking of the definite parity in broken SUSY or other isospectral family).

D. SUSY harmonic pair for binary switching

The parity-reversed contact with equally spaced and isospectral eigenspectra can be obtained by utilizing a harmonic potential, which satisfies the parity symmetry $\varepsilon(x) = \varepsilon(-x)$. Consider the harmonic potential $\varepsilon(x) = \varepsilon_b - \varepsilon_\Delta x^2$, which possesses the eigenvalues of $\gamma_m = -\varepsilon_b + (2m + 1)\varepsilon_\Delta^{1/2}/k_0$ and the eigenmodes

$$\psi_m(x) = \left(\frac{k_0\sqrt{\varepsilon_\Delta}}{\pi}\right)^{1/4} \frac{1}{\sqrt{2^m m!}} \dot{H}_m\left(\sqrt{k_0\sqrt{\varepsilon_\Delta}}x\right) e^{-\frac{1}{2}k_0\sqrt{\varepsilon_\Delta}x^2}, \quad (2)$$

where H_m is the m th-order Hermite polynomial ($m = 0, 1, \dots$). The SUSY transformation operator is then $A = (1/k_0)[\partial_x + k_0\varepsilon_\Delta^{1/2}x]$, which corresponds to the annihilation operator a [15]. The SUSY-partner potential becomes the shifted harmonic potential $\varepsilon_s(x) = \varepsilon_b - \varepsilon_\Delta x^2 - 2\varepsilon_\Delta^{1/2}/k_0$ with the eigenmode $\psi_s(x) = A\psi(x)$. At the same eigenvalue, the eigenmodes of the original harmonic potential and its SUSY partner satisfy the parity reversal for the zero modal overlap $\int \psi^*(x)(1/k_0)(\partial_x + k_0\varepsilon_\Delta^{1/2}x)\psi(x)dx = 0$, which is desired for complete block of wave transport in the *off* state.

We now assign the harmonic potential $\varepsilon_o(x) = \varepsilon_b - \varepsilon_\Delta x^2 = \varepsilon(-x)$ and its unbroken SUSY partner $\varepsilon_s(x) = \varepsilon_b - \varepsilon_\Delta x^2 - 2\varepsilon_\Delta^{1/2}/k_0$ as the output and input potential, respectively. Then, by exerting the index modulation

$\varepsilon_o(x) - \varepsilon_s(x) = 2\varepsilon_\Delta^{1/2}/k_0$ on one of the SUSY pair potentials for turning to the *on* state [Fig. 2(b), red arrow], complete overlaps between all the eigenmodes of input and output harmonic potentials are achieved with the breaking of the SUSY condition, deriving the equivalent transparency for all eigenmodes.

The landscapes of harmonic potentials are realized with optical waveguides that have finite widths. Figures 2(c) (*off* state) and 2(d) (*on* state) show the designed coupled silicon waveguides for the SUSY harmonic pair (y-axis propagation). To guarantee the parity reversal and uniform coupling for all eigenmodes, the harmonic waveguides are vertically aligned. Note that the waveguide which has the two-dimensional (z - x) cross section but maintains the single-mode condition along the z axis can be considered as a one-dimensional (x axis) spatially varying potential, with the effective potential landscape $\varepsilon(x)$ determined by the z -axis structural parameter.

Each waveguide, thus, has a spatially varying thickness $[t_o(x)$ for the original waveguide and $t_s(x)$ for its SUSY-partner waveguide; see Fig. S1 in Ref. [31]], and in spite of its finite width, 25 eigenmodes with almost equal level spacing are successfully obtained [Figs. 3(a) and 3(b)]. The control of the waveguide thickness $t_{o,s}(x)$, which can be achieved through the chip-integrable microfabrication for multiwedge structures [32], is just an example of harmonic potentials for the SUSY-based digital switching; a coupled system [33] or subwavelength design [34] can be considered an alternative.

E. Modal analysis

Figure 3(a) shows the effective modal index n_{eff} of residing eigenmodes for original and SUSY-partner waveguides before the coupling. Except for the annihilated ground state, 25 pairs of bound modes of the waveguides show perfect alignment in their eigenvalues, also satisfying the complete parity-reversal condition for the *off* state (red triangles for even parity and black inverted triangles for odd parity). The level spacing of n_{eff} in the original waveguide is almost uniform as $\Delta n_{\text{eff}} \sim 8.5 \times 10^{-3}$ [Fig. 3(b)]. We also note that the modal coupling between the switched waveguide and the SUSY waveguide is almost uniform for 25 eigenmodes, as shown in the level splitting by the coupling in Fig. 3(c).

With experimentally accessible potential modulation [16] of silicon to the original waveguide ($\Delta n = 8 \times 10^{-3} \sim \Delta n_{\text{eff}}$, for $\Delta n/n \sim 0.23\%$), the global parity- and phase-matching condition for the transparency (*on* state) is then achieved completely and simultaneously. The variation of the coupled eigenspectrum for the potential modulation Δn is shown in Fig. 3(d). Starting from the degenerate states at ‘‘ e ’’ having opposite parity [$\Delta n = 0$, Fig. 3(e)], the simultaneous matching of the parity and wave vector at ‘‘ f ’’ derives the ‘‘anticrossing’’ [$\Delta n = 8 \times 10^{-3} \sim \Delta n_{\text{eff}}$, Fig. 3(f)] accompanied with even-odd modal splitting. Notably, from the

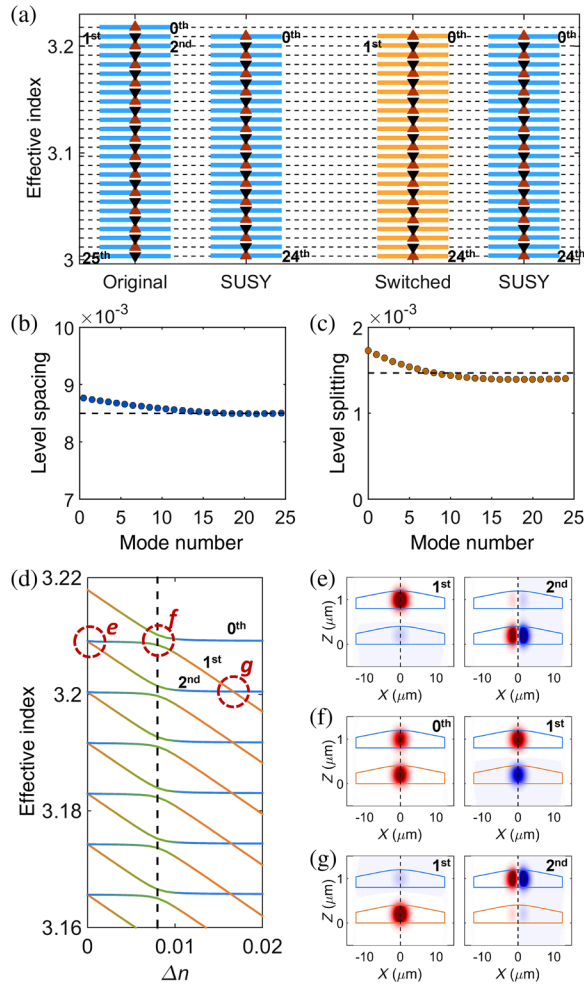


FIG. 3. Eigenmodes in the SUSY harmonic pair of silicon waveguides. (a) Effective modal indices n_{eff} of each waveguide before the coupling. (b) Level spacing of n_{eff} in the original waveguide. The black dashed line denotes $\Delta n_{\text{eff}} \sim 8.5 \times 10^{-3}$. (c) Level splitting by the coupling between the switched waveguide and the SUSY-partner waveguide. The black dashed line is the averaged splitting. (d) The variation of n_{eff} as a function of the refractive-index modulation Δn in the output waveguide. The e state denotes the degeneracy from the decoupling due to the parity reversal between eigenmodes. The f state (or g state) represents the anticrossing (or crossing) of eigenvalues. The modal profiles (E_x) for the states of e , f , and g in (d) are shown in (e), (f), and (g), respectively. All of the results are obtained by the full-wave eigenmode simulation in COMSOL MULTIPHYSICS.

identical overlap between eigenmodes in the original and SUSY waveguides, almost the same magnitude of the splitting is observed for all participating mode pairs. As we demonstrate with the “crossing” of eigenvalues at “ g ” and Fig. 3(g) ($\Delta n = 1.6 \times 10^{-2} \sim 2\Delta n_{\text{eff}}$), the global phase matching with parity reversal does not induce the coupling between input and output potentials (see Fig. S2 in Ref. [31] for other excited states).

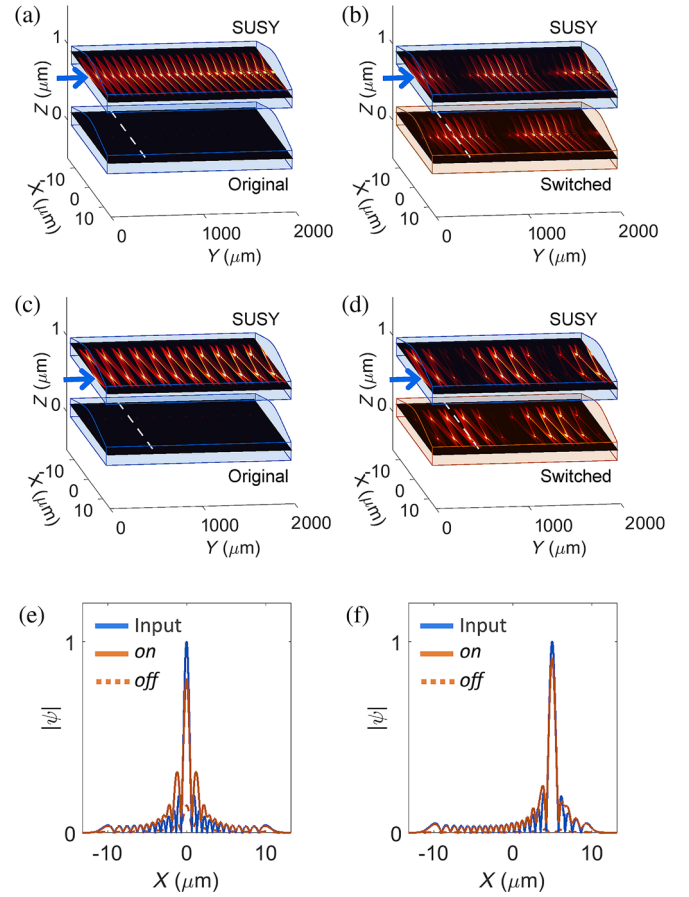


FIG. 4. Binary switching for point-source excitations in the SUSY harmonic pair. Light excitations (a),(b) at the center and (c),(d) 5- μm offset. (a),(c) *Off* state. (b),(d) *On* state. (e),(f) The reconstruction of the input wave front at the full coupling position in the output [white dashed lines in (a)–(d)]. The results are obtained by transfer-matrix calculations utilizing full-wave eigenmode simulations in COMSOL (Appendix B). All other parameters are the same as those in Figs. 2(c) and 2(d).

F. Point-source switching operation

Taking the 25 eigenmodes $\psi_m(x, z)$ in Fig. 3 as the basis in the modal expansion of switchable input waves, now we work on the static optical switching obtained from the coupled SUSY harmonic waveguide pair. We apply the transfer matrix from eigenmode simulations (Appendix B). Figure 4 shows the binary switching operation for point-source-like input waves. The input wave front is defined by the two-dimensional Gaussian function $\xi(x, z) = \exp[-(x - x_c)^2/(2\sigma_x^2) - (z - z_c)^2/(2\sigma_z^2)]$, where $\sigma_x = 10$ nm and $\sigma_z = 300$ nm ($z_c = 950$ nm) to construct the point-source excitation, without [$x_c = 0$, Figs. 4(a) and 4(b)] or with the x -axis offset [$x_c = 5$ μm , Figs. 4(c) and 4(d)]. Initially, the expansion and refocusing of wave fronts are observed periodically with the beat length of approximately $\lambda_0/\Delta n_{\text{eff}}$, while preserving the complete decoupling to the original output waveguide [Figs. 4(a) and 4(c), *off* state]. By exerting the potential modulation

$\Delta n = 8 \times 10^{-3} \sim \Delta n_{\text{eff}}$ on the output potential [orange waveguides in Figs. 4(b) and 4(d)], the *on* state from the directional coupling between input and output waveguides is achieved irrespective of the excitation position, also maintaining the periodic reconstruction of incident wave fronts [Figs. 4(e) and 4(f) each for $x_c = 0$ and $5 \mu\text{m}$]. This one-to-one spatial correspondence between input and output ports reflects high information capacity of the SUSY harmonic pair switch, also allowing the possibility of spatial switching techniques for random wave incidences.

G. Random wave switching operation

We work on the optical switching of the random waveform (Fig. 5). Specifically, for the arbitrary input $\xi(x, z)$, its guided part $\varphi(x, z) = \sum c_m \psi_m(x, z)$, where $c_m = \int \int \psi_m^*(x, z) \xi(x, z) dx dz$ will be switched by applying $\Delta n \sim \Delta n_{\text{eff}}$, independent of the phase or amplitude distributions of $\xi(x, z)$. Furthermore, from the equally spaced eigenspectrum of harmonic potentials deriving the reconstruction of wave fronts [33], we expect the lossless transfer of wave functions between optical elements.

In order to test completely random combinations of eigenmodes in terms of amplitude and phase, the input wave is set to be $\xi(x, z) = \sum u[0, 1] \exp[iu(0, 2\pi)] \psi_m(x, z)$ where $u[a, b]$ is the random number between a and b

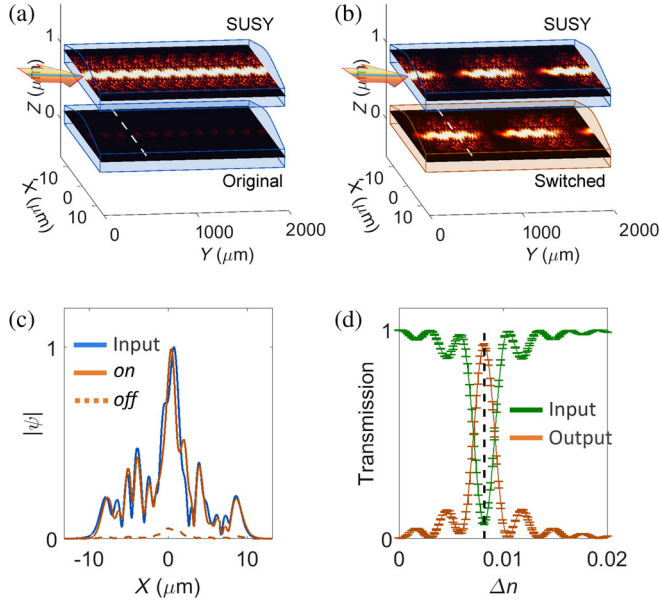


FIG. 5. Binary random wave switching in the SUSY harmonic pair: (a) *off* and (b) *on* states. (c) The reconstruction of the input wave front at the full coupling position in the output [dotted lines in (a),(b)]. (d) The power distribution in input and output waveguides at the full coupling position as a function of the modulation Δn . Error bar denotes the standard deviation for the ensembles of 400 random input waveform realizations. The results are obtained by transfer matrices linked with COMSOL eigenmode simulations (Appendix B). All other parameters are the same as those in Figs. 2(c) and 2(d).

following the uniform distribution. Even with the fully random input waves, the ideal transition from the decoupling [Fig. 5(a), *off* state] to directional coupling [Fig. 5(b), *on* state] is achieved through the moderate value of index modulation $\Delta n = 8 \times 10^{-3} \sim \Delta n_{\text{eff}}$, successfully deriving the even-odd-mode splitting and their interference. Most important, we demonstrate perfect transfer of spatial information [Fig. 5(c)] between optical elements, without *any* corruption.

To investigate the stability of the proposed binary switching, the statistical analysis is conducted for the ensemble of 400 random input waveform realizations [Fig. 5(d)]. High performance of the switching at $\Delta n = \Delta n_{\text{eff}}$ is demonstrated in terms of modulation depth (26 dB), power transfer (93%), and stability (1.1% error).

III. BUILDING BLOCK FOR FUZZY LOGICS

A. Design criteria

Extending the binary switching, we now challenge another solvable potential of the SUSY Pöschl-Teller [15] pair to realize the multilevel switching. Figures 6(a) and 6(b) show the schematics of the multilevel switching by using the SUSY Pöschl-Teller pair waveguide of sech^2 potentials. In the *off* state with the unbroken SUSY transformation from $V(x) = -(1/k_0) \partial_x \psi_0(x) / \psi_0(x)$, complete isolation from the isospectral parity reversal is achieved [Fig. 6(a)], the same as that in the SUSY harmonic pair. However, when the modulation increases with the Pöschl-Teller potential property which provides “linearly varying” eigenspectrum separation, the parity and wave-vector matching of the eigenmode is achieved “*in sequence*” from higher-order eigenmodes with the breaking of the SUSY relation [Fig. 6(b)]. We note that such a chain of eigenmodal “transparency” corresponds to the many-valued “truth,” while the “isolation” represents “false” [18].

B. SUSY Pöschl-Teller pair for multilevel switching

The Pöschl-Teller potential is realized with the permittivity of $\varepsilon(x) = \varepsilon_b + \varepsilon_\Delta \text{sech}^2(ax)$, which leads to the eigenvalues of $\gamma_m = -\varepsilon_b - (\alpha/k_0)^2 (p-m)^2$ [$m=0, 1, \dots, \text{floor}(p)$], where $p = -(1/2) + [(1/4) + (k_0/\alpha)^2 \varepsilon_\Delta]^{1/2}$. Note that the effective index $n_{\text{eff},(m)} = [\varepsilon_b + (\alpha/k_0)^2 (p-m)^2]^{1/2} \approx \varepsilon_b^{1/2} [1 + (\alpha/k_0)^2 (p-m)^2 / (2\varepsilon_b)]^{1/2}$ has the level separation varying linearly as $n_{\text{eff},(m)} - n_{\text{eff},(m+1)} = (\alpha/k_0)^2 (p-m-1/2) / \varepsilon_b^{1/2}$. The SUSY-transformation operator is $A = (1/k_0) [\partial_x + p \alpha \tanh(ax)]$, which derives the SUSY-partner potential of

$$\varepsilon_s(x) = \varepsilon_b + \left(\varepsilon_\Delta - \frac{2\alpha^2 p}{k_0^2} \right) \text{sech}^2(ax), \quad (3)$$

the modified Pöschl-Teller potential. Again, the eigenmodes of the original potential and its SUSY partner satisfy the parity reversal at the same eigenvalue.

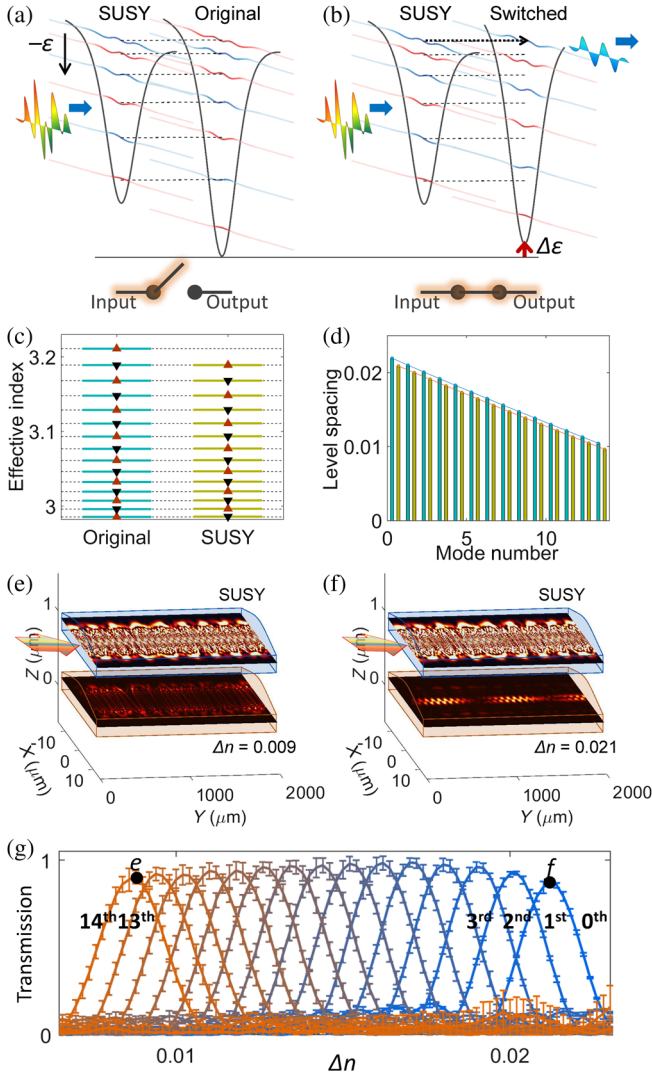


FIG. 6. Multilevel switching in the SUSY Pöschl-Teller pair. (a) The *off* state from the decoupling between the Pöschl-Teller potential (output) and its SUSY partner (input). (b) One of the many-valued *on* states from the coupling (black dotted arrow) through the modulated output (red arrow). (c) Effective indices n_{eff} of each waveguide before the coupling. (d) Level spacing of n_{eff} in the original [blue-green lines, $\varepsilon_o(x) = 8.6 + 1.7\text{sech}^2(5.5 \times 10^{-2}k_0x)$] and SUSY [red-brown lines, $\varepsilon_s(x) = 8.6 + 1.6\text{sech}^2(5.4 \times 10^{-2}k_0x)$] potentials. (e) The 14th truth ($\Delta n = 9 \times 10^{-3}$) and (f) zeroth truth ($\Delta n = 2.1 \times 10^{-2}$) transparency for random wave incidences. (g) The transmission of each eigenmode (zeroth to 14th) in the output waveguide at the full coupling position as a function of the modulation Δn . Error bar denotes the standard deviation for the ensembles of 400 random samples. All other parameters are the same as those in Fig. 2.

C. Switching operation

We design the Pöschl-Teller potential of $\varepsilon_o(x)$ and $\varepsilon_s(x)$, again by controlling the thickness of the silicon waveguides (Fig. S1 in Ref. [31]). The structures lead to

the isospectral eigenspectra [Fig. 6(c)], while maintaining the linear variation of the level separations [Fig. 6(d)]. Figures 6(e) and 6(f) denote the multilevel switching for different values of $\Delta n = 9 \times 10^{-3}$ and $\Delta n = 2.1 \times 10^{-2}$, respectively. For the random wave incidences $\xi(x, z)$, the degree of truth is determined by the transparent eigenmode [Fig. 6(e) for the 14th eigenmode and Fig. 6(f) for the ground state], which is determined by Δn . The stability of the multilevel switching is estimated with the ensemble of 400 random input waves for increasing Δn [Fig. 6(g)], confirming that the transparency of the eigenmode is achieved in sequence. We note that the mode-dependent transmission as a function of the modulation Δn derives the membership function in many-valued fuzzy logics [18,19] with uniform-level separations. The Pöschl-Teller pair with the overlap of eigenmode spectra then forms the building block of fuzzy logic systems, with high performance including the complete isolation at the *off* state and the utilization of optical bandwidth.

IV. CONCLUSION

In conclusion, we propose the collective switching of multimodes, allowing the dynamic control of random waves. In terms of footprint and waveform transparency, the realization of SUSY-based digital random wave switching boosts the performance of multimode-based signal processing for the chip-to-chip photonic circuits [35–37] by replacing multi-to-single-mode couplers and multiple single-mode switches. We note that the required level of the modulation depth $\Delta n/n \sim 0.23\%$ for the designed structure can be achieved with (10–40)-Gbps speed, utilizing the carrier density control in silicon, germanium, and their hybrid structures [16]. We emphasize that by decreasing the level separation in eigenspectra, all-optical modulations using optical nonlinearity [9,10,38] can be applied to the proposed SUSY-based building block for ultrafast switching applications. The many-valued feature in Pöschl-Teller SUSY pairs will also pave the way toward the optical realization of fuzzy logics [18,19].

Although we employ the SUSY pairs of parity-reversed isospectrality to the k domain in optics, the same concept can be extended to other wave platforms or the ω domain. For example, the isospectrality and harmonic realizations can be achieved in the ω domain to enable the lossless switching of temporally random waveforms by using coupled resonators [39] for multiresonant structures. Because of the generality of the Schrödinger equation, wave potentials for quantum-mechanical, elastic, and acoustic waves can also be envisaged as platforms for the proposed building blocks. The concept of mode-converted isospectrality can also be applied to other isospectral transformations, such as Householder transformation [40] between different dimensions or graph reduction [41].

ACKNOWLEDGMENTS

We acknowledge financial support from the National Research Foundation of Korea through the Global Frontier Program (Grant No. 2014M3A6B3063708), the Basic Science Research Program (Grant No. 2016R1A6A3A04009723), and the Korea Research Fellowship Program (Grant No. 2016H1D3A1938069), all funded by the Korean Government.

APPENDIX A: PARITY MIXING IN BROKEN SUSY AND ISOSPECTRAL FAMILY OF PARITY-SYMMETRIC POTENTIALS

Consider the parity-symmetric potential $\varepsilon(x) = \varepsilon(-x)$ and the SUSY-transforming operator $A = (1/k_0)\partial_x + V(x)$, where $V(x) = -(1/k_0)\partial_x\psi_d(x)/\psi_d(x)$ for $H\psi_d = \gamma_d\psi_d$. In the case of “broken” SUSY ($\gamma_d < \gamma_0$) [15,30], the mode of $\psi_d(x)$ is nodeless but unbounded (or non-normalizable) because γ_0 is the ground state. The signs of $\partial_x\psi_d(x)$ for $x \rightarrow \infty$ and $x \rightarrow -\infty$ are, thus, the same, and then $V(x)$ becomes the evenlike function (or zero Witten index [15]), in contrast to the case of unbroken SUSY: bounded $\psi_0(x)$, different signs of $\partial_x\psi_d(x)$ for $x \rightarrow \infty$ and $x \rightarrow -\infty$ and, thus, oddlike $V(x)$ (or unity Witten index [15]). Because the operator A for broken SUSY is the sum of the “odd-” parity operator $(1/k_0)\partial_x$ and “evenlike” parity operator $V(x)$, the application of the broken SUSY operator breaks the definite parity condition of the transformed eigenmode.

We can also introduce other sets of isospectral family [15,26] starting from the unbroken SUSY partner ($\gamma_d = \gamma_0$). From the unbroken SUSY Hamiltonian $H_s = AA^\dagger + \gamma_d$ with the SUSY optical potential $\varepsilon_s(x) = \varepsilon(x) + (2/k_0^2) \times \partial_x[\partial_x\psi_0(x)/\psi_0(x)]$, the Riccati equation for the SUSY potential has the form of $\partial_x V = -k_0 V^2 - k_0[\varepsilon_s(x) + \gamma_0]$.

Utilizing the particular solution of $V(x) = -(1/k_0)\partial_x\psi_0(x)/\psi_0(x)$, the general solution can be obtained as

$$V(x) = -\frac{1}{k_0} \frac{\partial_x\psi_0(x)}{\psi_0(x)} + \frac{\psi_0^2(x)}{c + \int_{-\infty}^x k_0\psi_0^2(x)dx}, \quad (\text{A1})$$

where c is an arbitrary constant ($c \rightarrow \pm\infty$ for the original unbroken case). From the superpotential $V(x)$ in Eq. (A1), other isospectral family potentials of $\varepsilon(x)$ can be obtained as $\varepsilon_f(x) = -V^2 + (1/k_0)\partial_x V - \gamma_0$. However, for the finite c and the even-parity ground state $\psi_0(x)$ from $\varepsilon(x) = \varepsilon(-x)$, the second term of Eq. (A1) breaks the definite parity condition of the transformed eigenmode by $A = (1/k_0)\partial_x + V(x)$. To summarize, in contrast to the parity conversion by unbroken SUSY transformation, broken SUSY or other isospectral family mix the parity of eigenmodes through the transformation.

APPENDIX B: TRANSFER-MATRIX METHOD USING EIGENMODE SIMULATIONS

First, by employing the full-wave eigenmodal simulation in COMSOL MULTIPHYSICS, all of the bounded eigenmodes $\psi_m(x, z)$ in SUSY waveguide structures can be derived with corresponding eigenvalues (effective index $n_{\text{eff-}m}$). From this complete eigenmode set for guided modes, we interpret the wave transport as the interfered propagation of each eigenmode that is excited by an incident wave.

Because the guided part of the arbitrary input waveform $\xi(x, z)$ at $y = 0$ is $\varphi(x, z) = \sum c_m \psi_m(x, z)$, where $c_m = \int \psi_m^*(x, z)\xi(x, z)dx dz$, the entire waveform $\Psi(x, z, y)$ is obtained as $\Psi(x, z, y) = \sum c_m \psi_m(x, z) \times \exp(-ik_0 n_{\text{eff-}m} y) = \sum \alpha_m(y) \psi_m(x, z)$, where

$$\begin{bmatrix} \alpha_0(y) \\ \alpha_1(y) \\ \vdots \\ \alpha_B(y) \end{bmatrix} = \begin{bmatrix} \exp(-ik_0 n_{\text{eff-}0} y) & 0 & \cdots & 0 \\ 0 & \exp(-ik_0 n_{\text{eff-}1} y) & 0 & \vdots \\ \vdots & \vdots & 0 & \ddots \\ 0 & \cdots & 0 & \exp(-ik_0 n_{\text{eff-}B} y) \end{bmatrix} \begin{bmatrix} c_0 \\ c_1 \\ \vdots \\ c_B \end{bmatrix}, \quad (\text{B1})$$

and B is the number of bounded excited states. The matrix in Eq. (B1) is the transfer matrix for bounded multimodes, and the entire three-dimensional waveform can be obtained by scanning the y axis with $\Psi(x, z, y) = \sum \alpha_m(y) \psi_m(x, z)$.

[1] B.G. Streetman and S. Banerjee, *Solid State Electronic Devices*, 5th ed. (Prentice-Hall, Englewood Cliffs, NJ, 2000).

[2] N. H. Wan, F. Meng, T. Schröder, R.-J. Shiu, E. H. Chen, and D. Englund, High-resolution optical spectroscopy using multimode interference in a compact tapered fibre, *Nat. Commun.* **6**, 7762 (2015).

[3] L. G. Wright, S. Wabnitz, D. N. Christodoulides, and F. W. Wise, Ultrabroadband Dispersive Radiation by Spatiotemporal Oscillation of Multimode Waves, *Phys. Rev. Lett.* **115**, 223902 (2015).

[4] M. Heinrich, M. A. Miri, S. Stutzer, R. El-Ganainy, S. Nolte, A. Szameit, and D. N. Christodoulides, Supersymmetric mode converters, *Nat. Commun.* **5**, 3698 (2014).

- [5] A.-L. Fehrembach, S. Hernandez, and A. Sentenac, k gaps for multimode waveguide gratings, *Phys. Rev. B* **73**, 233405 (2006).
- [6] H. R. Stuart, Dispersive multiplexing in multimode optical fiber, *Science* **289**, 281 (2000).
- [7] P. Li, X. Yang, T. W. Maß, J. Hanss, M. Lewin, A.-K. U. Michel, M. Wuttig, and T. Taubner, Reversible optical switching of highly confined phonon-polaritons with an ultrathin phase-change material, *Nat. Mater.* **15**, 870 (2016).
- [8] R. Ganesh and S. Gonella, From Modal Mixing to Tunable Functional Switches in Nonlinear Phononic Crystals, *Phys. Rev. Lett.* **114**, 054302 (2015).
- [9] M. Albert, A. Dantan, and M. Drewsen, Cavity electromagnetically induced transparency and all-optical switching using ion Coulomb crystals, *Nat. Photonics* **5**, 633 (2011).
- [10] K. Nozaki, T. Tanabe, A. Shinya, S. Matsuo, T. Sato, H. Taniyama, and M. Notomi, Sub-femtojoule all-optical switching using a photonic-crystal nanocavity, *Nat. Photonics* **4**, 477 (2010).
- [11] L.-W. Luo, N. Ophir, C. P. Chen, L. H. Gabrielli, C. B. Poitras, K. Bergman, and M. Lipson, WDM-compatible mode-division multiplexing on a silicon chip, *Nat. Commun.* **5**, 3069 (2014).
- [12] B. Stern, X. Zhu, C. P. Chen, L. D. Tzuang, J. Cardenas, K. Bergman, and M. Lipson, Integrated switch for simultaneous mode-division multiplexing (MDM) and wavelength-division multiplexing (WDM), [arXiv:1502.04692](https://arxiv.org/abs/1502.04692).
- [13] H. Subbaraman, X. Xu, A. Hosseini, X. Zhang, Y. Zhang, D. Kwong, and R. T. Chen, Recent advances in silicon-based passive and active optical interconnects, *Opt. Express* **23**, 2487 (2015).
- [14] G. Keiser, *Optical Fiber Communications*, 4th ed. (Wiley Online Library, New York, 2003), Chap. 11.
- [15] F. Cooper, A. Khare, and U. Sukhatme, *Supersymmetry in Quantum Mechanics* (World Scientific, Singapore, 2001).
- [16] G. T. Reed, G. Mashanovich, F. Gardes, and D. Thomson, Silicon optical modulators, *Nat. Photonics* **4**, 518 (2010).
- [17] C. Cecati, F. Ciancetta, and P. Siano, A multilevel inverter for photovoltaic systems with fuzzy logic control, *IEEE Transactions on Industrial Electronics* **57**, 4115 (2010).
- [18] T. J. Ross, *Fuzzy Logic with Engineering Applications* (John Wiley & Sons, New York, 2009).
- [19] L. A. Zadeh, Toward a theory of fuzzy information granulation and its centrality in human reasoning and fuzzy logic, *Fuzzy Sets Syst.* **90**, 111 (1997).
- [20] S. Longhi, Quantum-optical analogies using photonic structures, *Laser Photonics Rev.* **3**, 243 (2009).
- [21] M.-A. Miri, M. Heinrich, R. El-Ganainy, and D. N. Christodoulides, Supersymmetric Optical Structures, *Phys. Rev. Lett.* **110**, 233902 (2013).
- [22] S. Yu, X. Piao, J. Hong, and N. Park, Bloch-like waves in random-walk potentials based on supersymmetry, *Nat. Commun.* **6**, 8269 (2015).
- [23] R. Sapienza, P. Costantino, D. Wiersma, M. Ghulinyan, C. J. Oton, and L. Pavesi, Optical Analogue of Electronic Bloch Oscillations, *Phys. Rev. Lett.* **91**, 263902 (2003).
- [24] M. Kac, Can one hear the shape of a drum?, *Am. Math. Mon.* **73**, 1 (1966).
- [25] M.-A. Miri, M. Heinrich, and D. N. Christodoulides, Supersymmetry-generated complex optical potentials with real spectra, *Phys. Rev. A* **87**, 043819 (2013).
- [26] M.-A. Miri, M. Heinrich, and D. N. Christodoulides, SUSY-inspired one-dimensional transformation optics, *Optica* **1**, 89 (2014).
- [27] M. Heinrich, M. A. Miri, S. Stutzer, S. Nolte, D. N. Christodoulides, and A. Szameit, Observation of supersymmetric scattering in photonic lattices, *Opt. Lett.* **39**, 6130 (2014).
- [28] S. Yu, X. Piao, S. Koo, J. H. Shin, S. H. Lee, B. Min, and N. Park, Mode junction photonics with a symmetry-breaking arrangement of mode-orthogonal heterostructures, *Opt. Express* **19**, 25500 (2011).
- [29] V. G. Bagrov and B. F. Samsonov, Darboux transformation, factorization, and supersymmetry in one-dimensional quantum mechanics, *Theor. Math. Phys.* **104**, 1051 (1995).
- [30] A. A. Andrianov, N. Borisov, and M. Ioffe, The factorization method and quantum systems with equivalent energy spectra, *Phys. Lett.* **105A**, 19 (1984).
- [31] See Supplemental Material at <http://link.aps.org/supplemental/10.1103/PhysRevApplied.8.054010>, which includes the thickness of each SUSY pair and other excited states in the harmonic SUSY pair.
- [32] K. Y. Yang *et al.*, Broadband dispersion-engineered microresonator on a chip, *Nat. Photonics* **10**, 316 (2016).
- [33] R. Gordon, Harmonic oscillation in a spatially finite array waveguide, *Opt. Lett.* **29**, 2752 (2004).
- [34] B. Zhang, S. Brodbeck, Z. Wang, M. Kamp, C. Schneider, S. Höfling, and H. Deng, Coupling polariton quantum boxes in sub-wavelength grating microcavities, *Appl. Phys. Lett.* **106**, 051104 (2015).
- [35] R. Bruck, B. Mills, B. Troia, D. J. Thomson, F. Y. Gardes, Y. Hu, G. Z. Mashanovich, V. M. N. Passaro, G. T. Reed, and O. L. Muskens, Device-level characterization of the flow of light in integrated photonic circuits using ultrafast photomodulation spectroscopy, *Nat. Photonics* **9**, 54 (2015).
- [36] D. Dai, J. Bauters, and J. E. Bowers, Passive technologies for future large-scale photonic integrated circuits on silicon: Polarization handling, light non-reciprocity and loss reduction, *Light Sci. Appl.* **1**, e1 (2012).
- [37] C. Sun *et al.*, Single-chip microprocessor that communicates directly using light, *Nature (London)* **528**, 534 (2015).
- [38] S. Yu, X. Piao, and N. Park, Slow-light dispersion properties of multiatomic multiband coupled-resonator optical waveguides, *Phys. Rev. A* **85**, 023823 (2012).
- [39] P. Hamel, S. Haddadi, F. Raineri, P. Monnier, G. Beaudoin, I. Sagnes, A. Levenson, and A. M. Yacomotti, Spontaneous mirror-symmetry breaking in coupled photonic-crystal nanolasers, *Nat. Photonics* **9**, 311 (2015).
- [40] S. Yu, X. Piao, J. Hong, and N. Park, Interdimensional optical isospectrality inspired by graph networks, *Optica* **3**, 836 (2016).
- [41] L. Bunimovich and B. Webb, *Isospectral Transformations: A New Approach to Analyzing Multidimensional Systems and Networks* (Springer, New York, 2014).